

## REFERENCES

1. Filippov, A. F., Diffraction of an arbitrary acoustic wave by a wedge. *PMM Vol. 28, № 2, 1964.*
2. Gurevich, M. I., On the problem of a thin delta wing moving at a supersonic speed. *PMM Vol. 11, № 3, 1947.*
3. Tret'iakov, V. V., On the problem of reducing the solution of the wave equation in space to the solution of the Laplace equation, in the self-similar case. *Papers presented at the IVth All-Union Symposium on the propagation of elastic and elastoplastic waves, Kishinev, 1968.*

Translated by L. K.

UDC 534.121.014.2:538.601.155

**MODEL OF AN ELASTIC PLATE OF FINITE ELEMENTS IN SUPERSONIC FLOW**

PMM Vol. 39, № 1, 1975, pp. 86-94

V. A. VYSLOUKH, V. P. KANDIDOV and S. S. CHESNOKOV

(Moscow)

(Received November 20, 1973)

The dynamic stability of a thin plate in supersonic gas flow at low Strouhal numbers is examined. The aerodynamic forces are determined on the basis of the same partition mesh as for the representation of the plate as a model of finite elements. Rectangular elements with four coordinates at each node are used. The number of dynamical variables is diminished to one at each node as a result of reducing the order of the equation of motion. Examples of computing the plate vibrations in a vacuum and in fluid flow are presented.

Use of the finite-element method in aeroelasticity problems in the general case when the aerodynamic effects are determined numerically, is connected with great difficulties. This is related to the fact that a partition mesh not associated with the finite-element model representing the system is used to compute the aerodynamic forces. The aerodynamic mesh ordinarily consists of a comparatively large number of rhomboidal [1] or rectangular [2] cells and changes as the Mach number varies. The finite-element mesh has a larger spacing and is coupled rigidly to the structure. Changing it requires significant computational efforts.

It seems expedient to develop that approach to aeroelasticity problems in which the computation of the aerodynamic effects is performed on the basis of the same partition mesh as the description of the elastic-mass properties of the system. In order that an increase in the mesh spacing should not reduce the accuracy of the aerodynamic force calculation, the downwash within the limits of the cells is represented as a power series of the coordinates. The series coefficients are determined completely by the vector of the generalized coordinates of the element. Using the ordinary conjugate conditions of elements, the equation of motion of the elastic plate model in supersonic flow can be written in closed form without introducing a priori vibration modes

$$(K + \lambda^2 M)\mathbf{q} = \mathbf{Q}_a, \quad \mathbf{Q}_a = \sum_{n=0}^N \lambda^n A_n \mathbf{q} \quad (0.1)$$

Here  $\mathbf{q}$  is the vector of the generalized model coordinates,  $Q_a$  is the vector of the aerodynamic forces at the model nodes, and  $\lambda$  is a frequency parameter. The aerodynamic matrices of the model  $A_n$ , the stiffness  $K$  and mass  $M$  matrices are formed from the corresponding matrices of the separate elements with their mutual arrangement taken into account. The elements of the matrices  $A_n$  depend on the Mach number  $M_0$  and the flow velocity  $U$ . In the case of triangular elements, the method to obtain the matrices  $A_n$  has been developed in [3]. So-called matched elements, which have four generalized coordinates in each node, are often used in investigating the vibrations of thin plates. A fine partition mesh is needed in dynamics problems of inhomogeneous systems, hence, the order of the system (0.1) determined by the rank of the matrices  $M$  and  $A_n$  grows strongly while it is constrained by the size of the computer memory. This constraint is most essential in investigating nonconservative systems which require determination of the eigenvalues of non-Hermitian matrices.

One of the possible means of diminishing the order of the system (0.1), i. e. the number of dynamical variables of the model, without altering the partition mesh is proposed in [4]. It is based on introducing two systems of basis functions: "complete" to obtain the stiffness matrix  $K$  and "shortened" to obtain the mass matrix  $M$ .

This method is used herein to reduce the number of degrees of freedom of a model of matched elements in the dynamic stability problem of a plate in supersonic flow. The dynamical stability of a square cantiliver plate in gas flow with low Strouhal numbers is considered.

**1. Determination of the aerodynamic forces.** Within the framework of linear nonstationary supersonic flow theory, the fundamental equation for the perturbation potential  $\Phi(x, y, z, t)$  is [5]

$$(1 - M_0^2) \frac{\partial^2 \Phi}{\partial x^2} + \frac{\partial^2 \Phi}{\partial y^2} + \frac{\partial^2 \Phi}{\partial z^2} = \frac{2M_0}{c_0} \frac{\partial^2 \Phi}{\partial x \partial t} + \frac{1}{c_0^2} \frac{\partial^2 \Phi}{\partial t^2} \quad (1.1)$$

If the plate deformation is representable as  $z(x, y, t) = Z(x, y)e^{\lambda t}$ , where  $\lambda = \delta + i\omega$ ,  $c_0$  is the speed of sound, then the solution of (1.1) in the  $Z = 0$  plane is written as

$$\Phi(x, y, 0, t) = -\frac{1}{\pi} \int_{S(\xi, \eta)} \int W(\xi, \eta, t) (rs)^{-1/2} \times \exp\left[-\frac{\lambda M_0^2 (x - \xi)}{U\beta^2}\right] \operatorname{ch}\left[\frac{\lambda M_0 (rs)^{1/2}}{U\beta^2}\right] d\xi d\eta \quad (1.2)$$

$$\beta^2 = M_0^2 - 1, \quad r = (x - \xi) - \beta(y - \eta), \quad s = (x - \xi) + \beta(y - \eta)$$

Here  $W(\xi, \eta, t)$  is the downwash at the point  $\xi, \eta$  which is connected with the plate deflection mode by the relationship

$$W(\xi, \eta, t) = \left(\frac{\partial}{\partial t} + U \frac{\partial}{\partial \xi}\right) z(\xi, \eta, t) \quad (1.3)$$

The integration in (1.2) is over the area  $S(\xi, \eta)$  included in the reverse Mach cone with apex at the point  $x^*, y$ . Let us henceforth limit ourselves to the case of low Strouhal numbers  $k = \lambda L_x / U \ll 1$ , where  $L_x$  is the characteristic plate dimension along the flow direction. This permits expansion of the integrand in (1.2) in series. For low values of the Strouhal number ( $k \sim 0.1 - 0.2$  in practice) we can limit ourselves to first order terms in  $k$  by neglecting terms  $O(k^2)$  which correspond to the apparent masses.

The potential then becomes

$$\Phi(x, y, t) = \int_{S(\xi, \eta)} \int W(\xi, \eta, t) [G_0(\xi, \eta, x, y) + \lambda G_1(\xi, \eta, x, y) / U] d\xi d\eta \quad (1.4)$$

$$G_0 = -(rs)^{-1/2} / \pi, \quad G_1 = -M_0^2(x - \xi)G_0 / \beta^2$$

Piston theory can be used for  $M_0 k \gg 1$  and higher order terms in the expansion must be taken into account in (1.2) for  $k \sim 1$ .

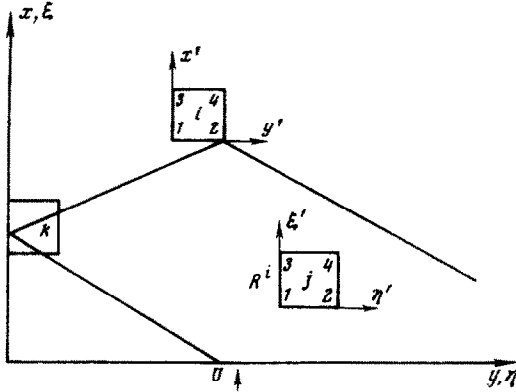


Fig. 1

Let us consider the model of a plate of finite elements. A plate divided into a number of rectangular elements with sides  $a^j, b^j$  is shown in Fig. 1. The intersections of the partition lines are called nodes. Let us take the mode of the displacement of an individual element in the form

$$z^j = \psi^T a w^j e^{\lambda t} \quad (1.5)$$

Here  $\psi(\xi', \eta')$  is a row of basis functions, and  $w^j$  is the vector of transverse displacements of the  $j$ th element.

Let us take the shortened system

$$\psi^T = \{1, \xi^*, \eta^*, \xi^* \eta^*\}, \quad (1.6)$$

$$\xi^* = \xi' / a^j, \quad \eta^* = \eta' / b^j$$

as  $\psi$ . Then

$$a = \begin{vmatrix} 1 & 0 & 0 & 0 \\ -1 & 1 & 0 & 0 \\ -1 & 0 & 1 & 0 \\ 1 & -1 & -1 & 0 \end{vmatrix}$$

According to (1.3), the downwash on the  $j$ th element becomes

$$W^j(\xi', \eta', t) = \left( U \frac{\partial \psi^T}{\partial \xi} + \lambda \psi^T \right) a w^j e^{\lambda t} \quad (1.7)$$

Substituting (1.7) into (1.4) and discarding second order terms, we obtain the perturbation potential at the point  $(x, y)$  associated with the downwash at the  $j$ th element

$$\Phi^{ij}(x, y, t) = \left( U \iint_{S^j} \frac{\partial \psi^T}{\partial \xi} G_0 d\xi' d\eta' + \lambda \iint_{S^j} \left( \psi^T G_0 + \frac{\partial \psi^T}{\partial \xi} G_1 \right) d\xi' d\eta' \right) a w^j e^{\lambda t} \quad (1.8)$$

after integrating over the area  $S^j(\xi, \eta)$  of the  $j$ th element. Setting  $x, y$  equal to the coordinates of nodes 1-4 of the  $i$ th element in (1.8), we obtain the potential vector at the nodes of the  $i$ th element which is due to downwash at the  $j$ th element (Fig. 1)

$$\Phi^{ij} = (UC^0 + \lambda a^j C^1) w^j \quad (1.9)$$

The elements of the matrices  $C^0, C^1$  are evaluated by the formulas

$$C_{11}^0 = -C_{12}^0 = -b^j \int_0^1 \int_0^1 (1 - \eta^*) G_0 d\xi^* d\eta^* \quad (1.10)$$

$$\begin{aligned}
 C_{l3}^0 &= -C_{l4}^0 = -b^j \int_0^1 \int_0^1 \eta^* G_0 d\xi^* d\eta^*, \quad G_0 = G_0(\xi_l^*, \eta_l^*, x_l, y_l) \\
 C_{l1}^1 &= b^j \int_0^1 \int_0^1 \left[ (1 - \xi^* - \eta^* + \xi^* \eta^*) G_0 - (1 - \eta^*) \frac{G_1}{a^j} \right] d\xi^* d\eta^* \quad (1.11) \\
 C_{l2}^1 &= b^j \int_0^1 \int_0^1 \left[ \xi^* (1 - \eta^*) G_0 + (1 - \eta^*) \frac{G_1}{a^j} \right] d\xi^* d\eta^* \\
 C_{l3}^1 &= b^j \int_0^1 \int_0^1 \left[ \eta^* (1 - \xi^*) G_0 - \eta^* \frac{G_1}{a^j} \right] d\xi^* d\eta^* \\
 C_{l4}^1 &= b^j \int_0^1 \int_0^1 \left[ \xi^* \eta^* G_0 + \eta^* \frac{G_1}{a^j} \right] d\xi^* d\eta^*, \quad G_1 = G_1(\xi_l^*, \eta_l^*, x_l, y_l)
 \end{aligned}$$

The subscript  $l$  here denotes the number of the row for elements of the matrices  $C$  and takes on the values 1, 2, 3, 4.

In determining the pressure  $p^{ij}(x, y)$  produced by the  $i$ th element, we assume that the potential within it is a linear combination of potentials of the nodal points

$$\Phi^{ij}(x', y', t) = \Psi^T a \Phi^{ije^{\lambda t}} \quad (1.12)$$

where  $x', y'$  is the local coordinate system of the  $i$ th element (Fig. 1), and  $\Psi(x', y')$  is the system of basis functions agreeing with (1.6). Substituting  $\Phi^{ij}(x', y', t)$  in the expression for the pressure [5] and taking account of (1.9), (1.12), we find

$$\begin{aligned}
 p^{ij}(x', y', t) &= 2\rho_0 \left( \frac{\partial}{\partial t} + U \frac{\partial}{\partial x} \right) \Phi^{ij}(x', y', t) = \quad (1.13) \\
 &2\rho_0 U \left[ U \frac{\partial \Psi^T}{\partial x} C^0 + \lambda \left( \Psi^T C^0 + \frac{\partial \Psi^T}{\partial x} C^1 \right) \right] \mathbf{w}^{je^{\lambda t}}
 \end{aligned}$$

Let us use the method of virtual work to evaluate the transverse force vector at the nodes  $\mathbf{P}_a^{ij}$ , equivalent to the load  $p^{ij}(x', y', t)$ . We take the displacement mode of the  $i$ th element in the form (1.5). Then

$$\mathbf{P}_a^{ije^{\lambda t}} = a^T \int \int_{S^i} \Psi(x', y') p^{ij}(x', y', t) dx' dy' \quad (1.14)$$

Substituting (1.13) into (1.14) and integrating over the area of the  $i$ th element, we obtain

$$\begin{aligned}
 \mathbf{P}_a^{ij} &= 2\rho_0 U \{ U d C^0 b^i + \lambda (d C^1 + e C^0) a^i b^i \} \mathbf{w}^j \\
 d &= \frac{1}{12} \begin{vmatrix} -2 & 2 & -1 & 1 \\ -2 & 2 & -1 & 1 \\ -1 & 1 & -2 & 2 \\ -1 & 1 & -2 & 2 \end{vmatrix}, \quad e = \frac{1}{36} \begin{vmatrix} 4 & 2 & 2 & 1 \\ 2 & 4 & 1 & 2 \\ 2 & 1 & 4 & 2 \\ 1 & 2 & 2 & 4 \end{vmatrix}
 \end{aligned}$$

We introduce the mutual aerodynamic stiffness  $B^{ij}$  and damping  $D^{ij}$  matrices for the  $i$ th element due to the motion of the  $j$ th element. Then

$$\mathbf{P}_a^{ij} = 2\rho_0 U (U b^i B^{ij} + \lambda a^i b^i D^{ij}) \mathbf{w}^j, \quad B^{ij} = d C^1, \quad D^{ij} = d C^1 + e C^0$$

The column of the total forces  $P_a^i$  acting at the nodes of the  $i$ th element is calculated by summation over the  $j$  elements which lie completely or partially in the reverse Mach cone. The Evvard theorem [5] on equivalent domains of integration which is valid for  $k \ll 1$  is used to compute the tip effect. For example, the integrands  $G_0(\xi, \eta, x, y)$  and  $G_1(\xi, \eta, x, y)$  in (1.10), (1.11) must be set equal to zero outside the domain  $R^i$  (see Fig. 1) in order to obtain the matrices  $B^{ik}$  and  $D^{ik}$  for the  $k$ th element lying partially within the Mach cone. Near the left edge of the plate  $R^i$  is given by the inequalities

$$\xi \leq -\beta|\eta - y| + x, \quad \xi \geq -\beta|\eta| + (x - \beta y)$$

In order to form the aerodynamic matrices  $B$  and  $D$  of the whole model, the forces  $P_a^i$  must be summed at the nodes of adjacent elements by using the continuity condition for the displacements. The resultant aerodynamic forces depend linearly on the vector of the nodal displacements  $w$  of the model

$$P_a = 2\rho_0 U^2 L_x B w e^{\lambda t} + 2\rho_0 U L_x L_y \lambda D w e^{\lambda t} \tag{1.15}$$

The integrals in (1.10) and (1.11) can be evaluated analytically, but it is more expedient to realize the whole algorithm to obtain the matrices  $B$  and  $D$  on a digital computer. The domain of integration over the elements lying partially in the domain  $R^i$  must be contracted for numerical integration in the relationships (1.10) and (1.11) in order to avoid the singularities in the integrands.

Let us consider a simple example of computing the aerodynamic forces, which will permit comparison between the approximate and the "exact" analytic solutions. Let a stiff rectangular plate with chord  $L_x = 1$  and the aspect ratio 2 perform harmonic oscillations around the leading edge  $x = 0$ , i. e.

$$z(x, t) = \alpha x e^{i\omega t} \tag{1.16}$$

The plate is divided into 6 elements along the chord, and 12 along the span. It is sufficient to consider the left half of the plate because of symmetry of the problem. The aerodynamic stiffness  $B$  and damping  $D$  matrices were computed on a digital computer for a flow at  $M_0 = \sqrt{2}$ . Substituting these matrices and the vector  $w(t)$  corresponding to the mode (1.16) into (1.14), we obtain values of the real and imaginary parts of the aerodynamic forces at the nodal points.

The results of the computation are represented in Fig. 2, where dimensionless values of the real  $P_1^*$  and the imaginary  $P_2^*$  parts of the nodal forces are plotted along the vertical axis. The numbers of partitions  $n$  parallel to the  $ox$ -axis are plotted along the

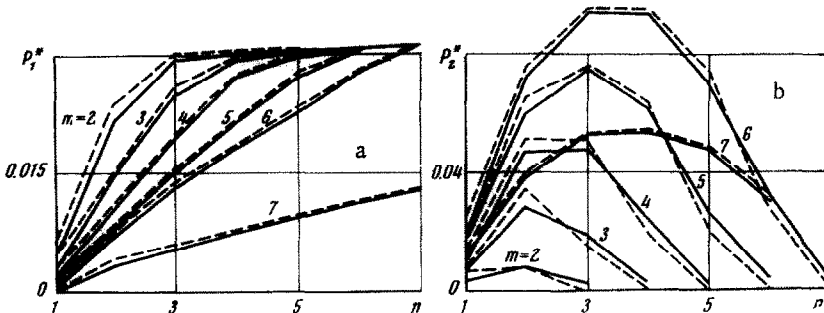


Fig. 2

horizontal axis in the graphs. The values of the forces are superposed by points for the nodes in the different sections perpendicular to the flow and are conventionally connected by a solid line. The numbers of these sections  $m$  are indicated beside the broken lines being formed.

The exact value of the nodal forces can easily be calculated for this example by proceeding from the analytical expression for the pressure. The downwash corresponding to the mode of the displacement (1.16) is  $W(\xi, \eta, t) = \alpha (U + \lambda \xi) e^{i\omega t}$ .

Substituting  $W(\xi, \eta, t)$  into (1.2), we obtain an analytic expression for the potential distribution

$$\Phi(x, y, t) = \begin{cases} -\frac{\alpha}{\pi} \left[ \frac{\pi x}{2} - xA + 2S + \lambda \left( -\frac{\pi x^2}{4} + \frac{x^2 A}{2} + (x - 2y) S \right) \right] e^{\lambda t}, & x > y \\ -\frac{\alpha}{\pi} \left[ \pi x - \lambda \pi \frac{x^2}{2} \right] e^{\lambda t}, & x \leq y \end{cases}$$

$$A = \arcsin \left( 1 - \frac{2y}{x} \right), \quad S = \sqrt{y(x-y)}$$

Hence

$$p(x, y) = \begin{cases} \frac{2\rho_0 U \alpha}{\pi} \left[ U \left( \frac{\pi}{2} - A \right) + 4\lambda S \right], & x > y \\ 2\rho_0 U^2 \alpha, & x < y \end{cases}$$

The exact values of the nodal forces equivalent to the pressure  $p(x, y)$  can be obtained by using (1.14). The corresponding values of the real and imaginary parts of the forces are presented in Fig. 2, where they are conventionally connected by dashes. The good agreement between the approximate and exact values of the nodal forces far from the plate edges and the satisfactory agreement near the leading and side edges are seen from a comparison of the curves. The accuracy of the calculations can be raised by increasing the number of elements.

Let us note that the values of the potential calculated at the model nodes agree with the exact values since the class of admissible displacements of the elements (1.5) includes the displacement mode (1.16) for the example considered. Deviation of the computed forces from the exact values is related to the representation of the potential within the element (1.12).

**2. Model of an elastic plate of matched elements.** Let us consider the  $i$ th element of the mesh shown in Fig. 1. We introduce three coordinates [6]  $\varphi$ ,  $\vartheta$ ,  $\tau$  in addition to the transverse displacement  $w$  at each node, in order to obtain its stiffness matrix  $K^i$ . These quantities form the vector of the generalized coordinates of an element with 16 components

$$\mathbf{q}^i = \text{col} \{w, \varphi, \vartheta, \tau\} \quad (2.1)$$

We take the deflection mode of an element  $z^{*i}$  in a form analogous to (1.5) by using the complete system of basis functions

$$\begin{aligned} z^{*i}(\xi^*, \eta^*, t) &= \chi^T(\xi^*, \eta^*) a^* \mathbf{q}^i e^{\lambda t} \\ \chi^T(\xi^*, \eta^*) &= \{\xi^{*l}, \eta^{*k}\}, \quad l, k = 0, 1, 2, 3 \end{aligned} \quad (2.2)$$

The number matrix  $a^*$  has the order  $16 \times 16$ .

Let us limit ourselves to the case of a homogeneous isotropic plate with bending stiffness  $D^0$ . The density of the elastic strain energy is

$$\varepsilon(\xi, \eta, t) = \frac{D^0}{2} \left[ \left( \frac{\partial^2 z^*}{\partial \xi^2} \right)^2 + \left( \frac{\partial^2 z^*}{\partial \eta^2} \right)^2 + \right. \\ \left. 2\nu \left( \frac{\partial^2 z^*}{\partial \xi^2} \right) \left( \frac{\partial^2 z^*}{\partial \eta^2} \right) + 2(1-\nu) \left( \frac{\partial^2 z^*}{\partial \xi \partial \eta} \right)^2 \right]$$

Substituting  $z^*$  in the form (2.2) we obtain

$$\varepsilon^i(\xi', \eta', t) = \frac{1}{2} \mathbf{q}^{iT} \mathbf{a}^{*T} E \mathbf{a}^* \mathbf{q}^i, \quad E(\xi, \eta) = D^0 \left[ \frac{\partial^2 \chi}{\partial \xi^2} \frac{\partial^2 \chi^T}{\partial \xi^2} + \right. \\ \left. \frac{\partial^2 \chi}{\partial \eta^2} \frac{\partial^2 \chi^T}{\partial \eta^2} + \nu \left( \frac{\partial^2 \chi}{\partial \xi^2} \frac{\partial^2 \chi^T}{\partial \eta^2} + \frac{\partial^2 \chi}{\partial \eta^2} \frac{\partial^2 \chi^T}{\partial \xi^2} \right) + 2(1-\nu) \frac{\partial^2 \chi}{\partial \xi \partial \eta} \frac{\partial^2 \chi^T}{\partial \xi \partial \eta} \right]$$

After integrating over the area  $S^i$  we find the elastic strain energy of an element which can be represented as follows:

$$V = \frac{1}{2} \mathbf{q}^{iT} K^i \mathbf{q}^i, \quad K^i = \mathbf{a}^{*T} \iint_{S^i} E(\xi, \eta) d\xi d\eta \mathbf{a}^*$$

The stiffness matrix  $K^i$  of an element governs the generalized force vector of the elastic strain  $\mathbf{Q}^i(t)$  conjugate to the vector  $\mathbf{q}^i(t)$

$$\mathbf{Q}^i = K^i \mathbf{q}^i, \quad \mathbf{Q}^i = \text{col} \{P_e, N_e, T_e, H_e\}$$

The components of the vector  $\mathbf{Q}^i$  are transverse elasticity  $P_e^i$  and moment  $N_e^i, T_e^i, H_e^i$  forces originating at the nodes of the element as it deforms.

We use the shortened system of basis functions  $\psi(\xi, \eta)$  to obtain the mass matrix  $M^i$  of the element by taking the displacement mode in the form (1.5). Then the density of the inertial forces on the element are

$$p_m^i = -\lambda^2 \rho h \psi(\xi', \eta') a w e^{\lambda t} \quad (2.3)$$

Here  $\rho$  is the material density, and  $h$  is the plate thickness. Substituting (2.3) and (1.14) and integrating over the area of the  $i$ th element, we obtain the vector of the inertial forces at the nodes ( $M^i$  is a  $(4 \times 4)$  matrix of the element mass)

$$P_m^i = -\lambda^2 M^i \mathbf{w}^i, \quad M^i = \mathbf{a}^T \iint_{S^i} \rho h \psi \psi^T d\xi d\eta \mathbf{a}$$

The conjugate conditions of the elements expounded in Sect. 1, are supplemented by requirements of continuity of the variables  $\varphi, \vartheta, \tau$  at the nodes in the case of an elastic plate. It is important to note that not only the continuity but also the smoothness of the deflection mode on the boundary of adjacent elements are assured upon compliance with the requirements mentioned. In this connection, the elements with the generalized coordinate (2.1) are called matched elements. Using the conjugate conditions, we can form the generalized coordinate vector  $\mathbf{q}$  of the model.

Writing the condition of equivalence of the forces  $P_a, P_e, P_m$  and of the moments  $N_e, T_e, H_e$  at each node, we obtain a system of four matrix equations

$$K^{pw} \mathbf{w} + K^{p\varphi} \boldsymbol{\varphi} + K^{p\vartheta} \boldsymbol{\vartheta} + K^{p\tau} \boldsymbol{\tau} + \lambda^2 M \mathbf{w} + \\ 2\rho_0 U^2 L_x B \mathbf{w} + 2\rho_0 \lambda U L_x L_y D \mathbf{w} = 0 \\ K^{Nw} \mathbf{w} + K^{N\varphi} \boldsymbol{\varphi} + K^{N\vartheta} \boldsymbol{\vartheta} + K^{N\tau} \boldsymbol{\tau} = 0 \\ K^{Tw} \mathbf{w} + K^{T\varphi} \boldsymbol{\varphi} + K^{T\vartheta} \boldsymbol{\vartheta} + K^{T\tau} \boldsymbol{\tau} = 0 \\ K^{Hw} \mathbf{w} + K^{H\varphi} \boldsymbol{\varphi} + K^{H\vartheta} \boldsymbol{\vartheta} + K^{H\tau} \boldsymbol{\tau} = 0 \quad (2.4)$$

Here  $K^{pw}$  is a  $(R \times R)$  sector of the stiffness matrix which describes the connection between the transverse forces  $P_e$  and the displacements  $w$ ,  $K^{p\phi}$  between the forces  $P_e$  and the angles  $\phi$  etc., and  $R$  is the number of free nodes of the model.

It is seen from the system (2.4) that the variables  $\phi$ ,  $\theta$ ,  $\tau$  can be expressed linearly in terms of  $w$ . After matrix transformations such as those expounded in [4], the system (2.4) can be reduced to the following form:

$$K^*w + \lambda^2 Mw + 2\rho_0 U^2 L_x Bw + 2\rho_0 U \lambda L_x L_y Dw = 0 \quad (2.5)$$

where  $K^*$  is the reduced stiffness matrix.

Consequently, the order of the matrix equation of motion of the model has been reduced fourfold and becomes equal to the number of free nodes  $R$ .

**3. Examples of the computation.** To estimate the accuracy of the solution when using the proposed reduction of the number of degrees of freedom, let us consider the free vibrations of a square cantiliver plate with the edge length  $L = 0.24$  m. The remaining plate parameters are: Young's modulus  $E = 1.96 \times 10^{11}$  N/m<sup>2</sup> (steel), Poisson's ratio  $\nu = 0.3$ ,  $\rho = 7.8 \times 10^3$  kg/m<sup>3</sup> and  $h = 0.00227$  m.

Values of the circular frequencies  $\omega$  for a plate model from matched elements with  $(3 \times 3)$ ,  $(4 \times 4)$  and  $(5 \times 5)$  partitions, calculated by using a computer, are presented in Table 1, which also shows the frequencies of a model of unmatched elements with shortened mass matrices [4] and experimental data [7].

Table 1

tone	matched elements			unmatched elements			
	3 × 3	4 × 4	5 × 5	3 × 3	4 × 4	5 × 5	experiment
1	205.0	206.6	207.2	205.4	206.6	206.8	208.4
2	512.9	511.1	510.5	514.1	511.7	511.1	510.5
3	1342.3	1324.4	1308.8	1379.9	1343.5	1320.8	1280.2
4	1778.8	1730.4	1696.9	1766.8	1720.2	1689.8	1639.6

The good agreement of the frequencies obtained for the matched elements to the experimental data is seen from the table. The example presented illustrates the efficiency of reducing the number of degrees of freedom in the case of matched elements.

The dynamic stability of the plate under consideration is investigated for the case of a flow incoming along the clamped side. A model of  $(5 \times 5)$  square matched elements is selected for the computation. It has 30 degrees of freedom and assures no worse than 3, 5% accuracy in the determination of the first four vibration frequencies in a vacuum. The aerodynamic matrices describing the effect of the supersonic flow were calculated for a number of Mach number values without taking account of aerodynamic damping. The eigenvalues  $\lambda = \delta + i\omega$  of (2.5) were determined for various flow velocities by using a digital computer.

The behavior of  $\lambda$  as the velocity changes is usually considered in the complex plane. As the flow velocity increases, the eigenvalues of the first two vibration tones  $\lambda_1$  and  $\lambda_2$  move along the  $\omega$ -axis while remaining pure imaginary. Starting with some velocity, the  $\lambda_1$  and  $\lambda_2$  converge. Finally, they become complex for the critical value  $M_0^* = 3.1$ ; the imaginary parts of  $\lambda_1$  and  $\lambda_2$  agree, and the real parts differ in sign. The values of the frequencies  $\omega_1$  and  $\omega_2$  are presented below for various  $M_0$



$M_0 = \sqrt{2}$	2.3	2.8	2.9	3.0	3.1
$\omega_1 = 239.9$	251.0	263.8	268.3	289.0	317.8
$\omega_2 = 356.8$	397.6	385.6	379.3	352.9	317.8

When using piston theory, the loss of stability occurs at lower values of  $M_0$ , hence, the critical frequencies are higher. Thus, the values  $M_0^* = 2.96$ ,  $\omega^* = 386.9$  are obtained by the finite element method in [8], and the values  $M_0^* = 2.78$ ,  $\omega^* = 384.6$  by the Ritz method in [9]. This difference is apparently explained by the tip effect on the free edge parallel to the clamped edge of the plate.

The amplitude and phase distributions of the vibrations at various points of the plate can be obtained with the aid of the eigenvectors calculated from (2.5), and the physical picture of the loss of stability can be explained.

The authors are grateful to S.P. Strelkov for continued attention to the research and for useful discussions.

#### REFERENCES

1. Belotserkovskii, S. M., Skripach, B. K. and Tabachnikov, V. T., Wing in a Nonstationary Gas Flow. "Nauka", Moscow, 1971.
2. Bisplinghoff, R. L. and Ashley, H., Principles of Aeroelasticity. Wiley, New York, 1962.
3. Kari-Appa, Kinematically consistent unsteady aerodynamic coefficients in supersonic flow. Intern. J. Numer. Meth. Engng., Vol. 7, №2, 1973.
4. Vysloukh, V. A., Kandidov, V. P. and Chesnokov, S. S., Reduction of the degrees of freedom in solving dynamic problems by the finite element method. Intern. J. Numer. Meth. Engng., Vol. 7, №2, 1973.
5. Bisplinghoff, R. L., Ashley, H. and Halfman, R. L., Aeroelasticity. Izd. Inostr. Lit., Moscow, 1958.
6. Carson, W. G. and Newton, R. E., Plate buckling analysis using a fully compatible finite element. AIAA Journal, Vol. 7, №3, 1969.
7. Barton, M. V., Vibrations of rectangular and skew cantilever plates. J. Appl. Mech., Vol. 18, №2, 1951.
8. Marchenko, G. A., Ritz method in nonconservative problems of elastic stability theory. Izv. VUZ, Aviats. Mekh., №3, 1966.
9. Kandidov, V. P. and Chesnokov, S. S., Analysis of the stability of rectangular plates in an air flow by the finite element method. Vestnik Mosk. Univ., Ser. Fiz. -Astron., №5, 1972.

Translated by M. D. F.